Functional Materials 13, No.4 (2006)

Conductivity anisotropy and pseudogap state evolution in $HoBa_2Cu_3O_{7-\delta}$ single crystals of a preset flat defect topology at decreasing oxygen concentration

M.A.Obolenskii, R.V.Vovk, A.V.Bondarenko, I.L.Goulatis

V. Karazin Kharkiv National University, 4 Svobody Sq., 61077 Kharkiv, Ukraine

Received April 4, 2006

The temperature dependences of electrical resistance along the **c**-axis and in the ab plane for $HoBa_2Cu_3O_{7-\delta}$ single crystals with various oxygen content have been measured. The temperature dependences of the pseudogap value have been determined. These dependences have been shown to be described satisfactorily within the frame of crossover (BCS-BEK) theory. The intensification of localization effects results in depression of the pseudogap state. A considerable anisotropy of the superconductive properties has been observed when measuring the temperature dependences of electrical resistance along and across the basis plane.

Измерены температурные зависимости электропроводности вдоль оси **c** и в *ab*-плоскости монокристаллов $HoBa_2Cu_3O_{7-\delta}$ с различным содержанием кислорода. Определены температурные зависимости величины псевдощели. Показано, что эти зависимости удовлетворительно описываются в рамках теории кроссовера БКШ-БЭК. Усиление эффектов локализации приводит к подавлению псевдощелевого состояния. Обнаружена значительная анизотропия сверхпроводящих свойств при измерениях температурных зависимостей электросопротивления вдоль и поперек базисной плоскости.

It is well known that the change of the oxygen and impurity concentrations in high-temperature superconducting compounds (HTSC) influences substantially the current carrier density, the material thermal and electrical conductivity [1, 2]. Recently, the realization of pseudogap state (PG) anomalies arising in the "underdoped" HTSC compositions with lower current carrier concentration than the optimum one (see, e.g., [3–5]). According to modern concepts, there are two main scenarios for the onset of the PG anomalies in HTSC systems. According to the first scenario, the PG appearance is related to "dielectric" type short-range order fluctuations, e.g., the anti-ferromagnetic fluctuations, spin and charging density waves, etc. (see [3] for a review). The second scenario supposes the formation of Cooper pairs already at temperatures substantially exceeding the critical one, $T^* >> T_c$, followed by the establishment of their phase coherence at $T < T_c$ [4, 5]. Despite the extensive experimental material collected until now, this question remains still undetermined. Within this aspect, the most promising materials to study are compounds of the $ReBa_2Cu_3O_{7-\delta}$ system (Re = Y or other rare-earth ion), that is due to the acquired knowledge in single crystals production technology and the relatively easy way to replace yttrium with its isoelectron rare-earth analogues. This, in turn, makes it possible to vary the compound conductivity characteristics by partial or complete substitution of its components. In this work, we report the results concerning the PG value evolution and temperature depend-

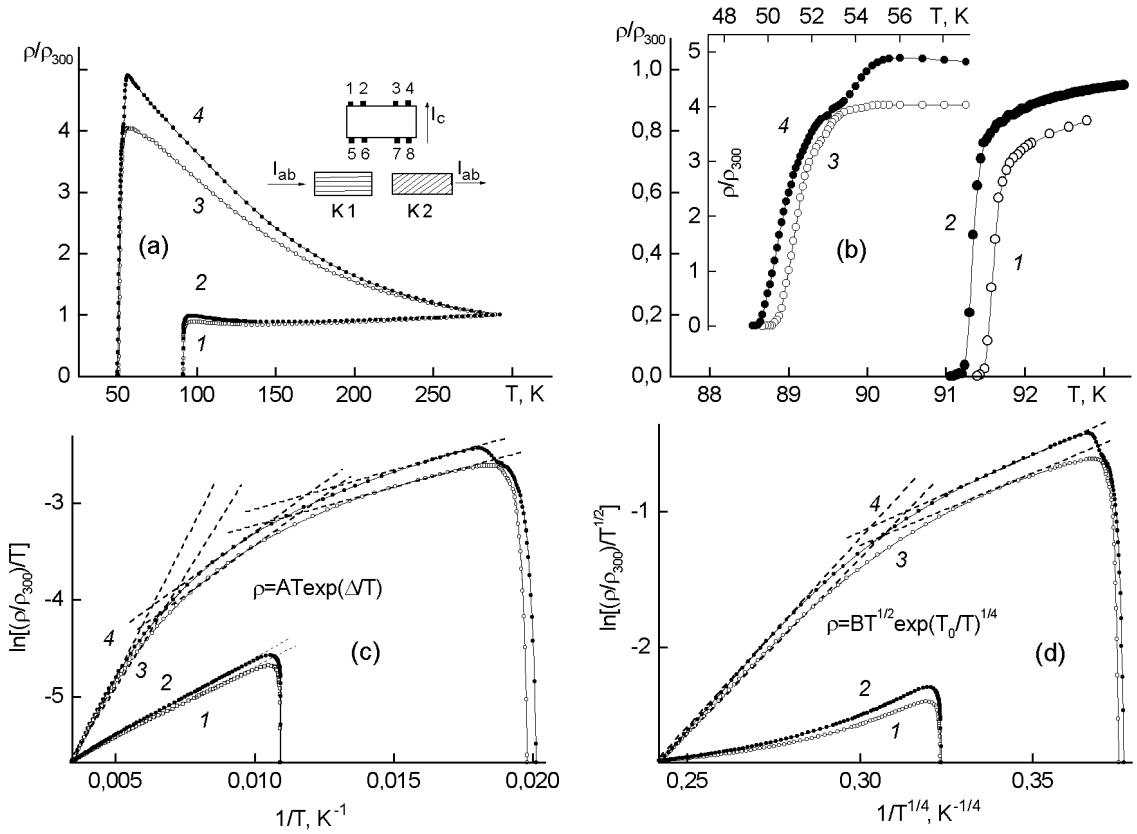

Fig. 1. Temperature dependences $\rho_c(T)$ along **c**-axis in coordinates ρ/ρ_{300} — T (a); $\ln[(\rho/\rho_{300})/T]$ – $1/T$ (c); $\ln[(\rho/\rho_{300})/T^{1/2}]$ – $1/T^{1/4}$ (d). The resistive transitions to the superconducting state are shown in Fig. 1(b). The open symbols for K1 crystal data, the full ones, to the K2. The *1*, *2* and *3*, *4* curves are measured prior to and after reduction of the oxygen content, respectively. In the inset the experiment geometry is shown schematically.

ence (that have been obtained by measuring the conductivity in the *ab*-plane and the energy charge transfer gaps along **c** axis), in oxygen doped $HoBa_2Cu_3O_{7-\delta}$ single crystals at decreasing oxygen content.

The $HoBa_2Cu_3O_{7-\delta}$ single crystals were grown in a gold crucible by self-flux method similar to $YBa_2Cu_3O_{7-\delta}$ single crystals synthesis technology described in detail in [1]. For the resistivity measurements, the single crystals of $2\times1.8\pm0.5$ mm^3 (Sample K1) and $1.9\times1.9\times0.5$ mm^3 (Sample K2) sizes were selected with the **c** axis oriented along the smallest dimension. The experimental geometry was selected so that the transport current vector was different from the twin boundaries (TB) orientation in the *ab*-plane, as is shown in the inset of Fig. 1(a). The electric contacts were formed according to the standard four-contact scheme by applying silver paste onto the crystal surface and the connection of gold conductors (0.05 mm in dia.). This procedure provided a contact transition resistance of less than 1 Ω. The electric resistance in the *ab*-plane and along **c**-axis was measured using the standard method for two opposite directions of a dc current up to 10 mA, as it was described in detail in [1]. To obtain samples with an optimum oxygen content and high T_c, the crystals were annealed in oxygen flow at 420°C for 3 days. To decrease the oxygen content, the crystals were annealed in vacuum at 500°C. The parameters and the data obtained for the samples are given in Table. The temperature was measured by a copper-constantan thermocouple. All the measurements were carried out three days after annealing, thus providing an equilibrium oxygen distribution over the sample volume, at room temperature [2].

The $\rho_c(T)$ dependences measured prior to and after the sample annealing at different temperatures are shown in Fig. 1(a). The resistive transitions to the superconductive state are shown in Fig. 1(b). It can be noticed that as the oxygen concentration is reduced, ρ_c increases, T_c decreases and the

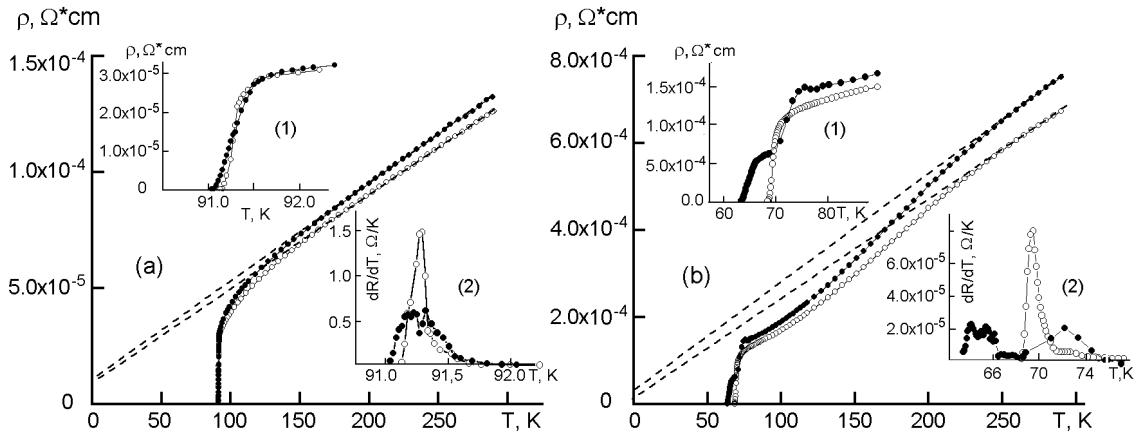

Fig. 2. Temperature dependences of the electric resistance in the *ab*-plane $\rho_{ab}(T)$ for the K1 crystal (open symbols) and for the K2 crystal (full symbols) measured prior to (a) and after (b) the the oxygen content reduction. Insets show the resistive transitions into the superconducting state in R — T coordinates: [(a)–(1)]; [(b)–(1)] and in dR/dT – T coordinates: [(a)–(2)] and [(b)–(2)].

$\rho_c(T)$ curves show a transition from the metallic behavior to that with a characteristic semiconductor deflection. In Figs. 1(c) and 1(d), the same dependences are shown in coordinates $\ln(\rho_c/T) - 1/T$ and $\ln(\rho_c/T^{1/2}) - 1/T^{1/4}$, that correspond to the description of $\rho_c = f(T)$ function by means of analytical expressions:

$$\rho_c = A\,T\exp(\Delta_c/T), \qquad (1)$$

$$\rho_c = BT^{1/2}\exp(T_0/T)^{1/4}, \qquad (2)$$

where A, B, and T_0 are constants and Δ_c is the activation energy. It is known that the first expression is typical for the activation mechanism of the carrier motion, while the second one is typical for the hopping conductance with a variable hopping length. It is seen from the Figure that for samples with optimum oxygen composition, the $\rho_c(T)$ dependence of is better fitted by the Eq.(1), while for oxygen-deficient samples, the dependences are better described by Eq.(2). It is also seen from the Figure that the slope of the curves increases with the increasing oxygen deficiency, which, in turn, means that the activation energy also increases (see Table). It is also to note that the slope of the curve corresponding to the minimum $T_c \approx 70$ K changes more than twice at 155 K and 88 K, what, in turn, corresponds to the activation energy change from 48 to 15 and to 7.7 meV, respectively, and reflects the presence of phase transitions observed before [1] for YBaCuO single crystals. According to [1], such phase transitions affect the charge transport kinetics. Thus, the consideration of the experimental data obtained allows us to suppose that the decreasing oxygen content results in localization of the carriers

Table. Parameters of experimental samples

Sample \ Parameters		**c**-axis				ab-plane				
		T_c, K	Δ_c, meV			ρ(300), μΩ·cm	T_c, K	T^*, K	Δ^*_{max}, meV	$\xi_c(0)$, Å
			$T <$ 88 K	88 K $< T <$ 155 K	$T >$ 155 K					
K1 (I‖TB)	Initial	91.5	12.67			120	91.3	188	68.02	1.88
	Annealed	51.37	45.25	14.14	5.52	673	69.51	270	17.93	4.23
K2 ($\alpha_{I,TB} = 45°$)	Initial	91.8	13.88			125	$T_{c_1} = 91.33$ $T_{c_1} = 91.23$	185	69.91	1.77
	Annealed	50.4	47.75	15.09	7.67	695	$T_{c_1} = 72.18$ $T_{c_1} = 64.18$	256	19.22	4.18

along the **c**-axis direction and in a modification of the layer interaction.

In Fig. 2, shown are the temperature dependences of the electric resistance in the *ab*-plane, $\rho_{ab}(T)$, for the same samples, measured prior to (a) and after (b) the oxygen content reduction. A principal behavior difference of these dependences is seen as compared to those observed when measuring the temperature dependence of electrical resistance perpendicular to the basis plane. While the oxygen stoichiometry deflection results in a metal/semiconductor transition for the $\rho_c(T)$ curves related to the basic plane, the linear $\rho_{ab}(T)$ dependences are maintained within a considerable range of rather high temperatures. This, according to NAFL [6], evidences reliably the normal system state. At further temperature decreasing below a certain characteristic value T^*, a deviation of $\rho_{ab}(T)$ from the linear dependence occurs, which evidences the presence of some excess conductivity that may be caused by transition to the pseudogap (PG) regime, that will be considered in detail below.

It is seen from Table and Fig. 2(b) that as oxygen concentration decreases, the critical temperature decreases, the absolute value of electric resistance increases and the area of the linear $\rho_{ab}(T)$ dependence narrows significantly. The small width of the superconducting transition ($\Delta T_c \leq 0.5$ K) increases considerably, and for the K2 sample the transition acquires a step-like character which evidences obviously the occurrence of two phases in the sample with different superconductive transition critical temperatures. Because such a wide bottom step was not observed in the measurements of K1 sample (**I** ∥ TB) (open symbols), it is logical to explain its existence in the first case by the superconductivity suppression at TB. The above is confirmed by a clearly defined step-like form of the superconducting (SC) transition obtained from the $\rho_c(T)$ measurements in the same K2 crystal along **c**-axis (Fig. 1(b)). In fact, the pronounced step presence in the $\rho_{ab}(T)$ implies the presence of percolation paths for the transport current in the high-temperature phase when **I**∥TB∥**c** and their absence when the angle between **I** and TB is 45°. It should be also noted that such a feature in the SC transition was shown for the K2 crystal even before oxygen depletion (T_c = 90 K) as two clear peaks in the $dR(T)/dT$ dependences (inset (2) in Fig. 1(a)). The width increase for both the peaks under oxygen deficiency (inset (2) in Fig. 1(b)) shows that the difference between the critical temperatures of the low-and high-temperature superconducting phases T_{c1} and T_{c2} increases (see Table).

A second important feature of the electric resistivity temperature dependences for the samples with low T_c consists in a significant (about 20 K) difference between the critical temperatures measured along the basic plane and perpendicular thereto. Such an effect was observed in $Bi_2Sr_3Ca_xCu_2O_{8+x}$ [7] and $YBa_2Cu_3O_{7-\delta}$ [8] single crystals with a large deflection from oxygen stoichiometry during the resistivity and magnetic susceptibility measurements. The authors [8] explained the effect by the realization of Fridel transition in the sample [9], which consists in the transversal superconductivity suppression within a temperature range under the critical $T_f < T < T_c$ (T_f — Fridel temperature) due to a specific mechanism of Josephson vortice growth in layered superconductors. As it was shown in theoretical work [10], the realization of such mechanism in real crystal is possible in case of some disruption in periodical distribution of conducting layers. The observed effect seems to result also from the sample inhomogeneity, for example, from the superconductivity suppression at TB. However, taking under consideration the experimental geometry, we can conclude that this is not the governing factor in the observed T_c anisotropy. In fact, as is seen from Table, when the transport current passes both along and across the TB in basic plane, the significant difference is maintained between the critical temperature values measured along **c** axis and in *ab*-plane, including the T_{c1} and T_{c2} values observed for both peaks in $dR(T)/dT$ dependences. According to [8], a periodicity disruption in the conductive layers distributions could be due to the existence of layers with different T_c within the sample, separated from each other. This scenario is evidenced by results [2] which demonstrate that the oxygen concentration reduction in $YBa_2Cu_3O_{7-\delta}$ single crystals causes the conducting subsystem disintegration into several phases with different T_c. The existence of similar phases is not observed often during the resistivity SC transitions measured in the *ab*-plane due to percolation paths of the transport current in the phase with maximum T_c (like it is in case when **I**∥TB∥**c** — open symbols in the insets (1) and (2) in Fig. 2).

As it was above mentioned, below a certain characteristic temperature T^*, the $\rho_{ab}(T)$ dependences become "rounded"; perhaps this fact might be due to the appearance of an excess conductivity determined by the relationship

$$\Delta\sigma = \sigma - \sigma_0, \qquad (3)$$

where $\sigma_0 = \rho_0^{-1} = (A + BT)^{-1}$ is the conductivity value determined by extrapolating the linear section to zero temperature and $\sigma = \rho^{-1}$ is the experimental conductivity in the normal state. The temperature dependences of the excess conductivity in $\ln\Delta\sigma - 1/T$ and $\Delta\sigma - T$ (inset (a)) coordinates are shown in Fig. 3. It is seen that these dependences are linear in a wide temperature interval, in agreement with the expression:

$$\Delta\sigma \sim \exp(\Delta^*_{ab}/T) \qquad (4)$$

where Δ^*_{ab} is a quantity defining a certain thermo-activation process across the energy gap, also called "pseudo-gap" (PG). As it is seen from Table, the PG value calculated from (4), reduces from 70 to 18 meV with decreasing oxygen concentration. Thus, a clear correlation exists in the evolution of the PG value Δ^*_{ab} in the basic plane and the energy gap of charge transfer along the **c** axis direction Δ_c, as oxygen concentration varies. The Δ^*_{ab} value decreases while Δ_c increases, and vice versa. Thus, the analysis of the obtained experimental data allow us to conclude the PG-regime suppression at a simultaneous amplification of the localization effects.

The exponential dependence $\Delta\sigma(T)$ was observed in YBaCuO ceramics [11], films [5], and manganese doped samples [12], with comparable Δ^* values. As shown in [5], the experimental data approximation could be extended significantly by introducing the $(1 - T/T^*)$ factor. In this case, the excess conductivity is proportional to the density of superconducting carriers $n_s \sim (1 - T/T^*)$ and in inverse proportion to the number of pairs $\sim\exp(-\Delta^*/kT)$ destroyed by thermal motion:

$$\Delta\sigma \sim (1 - T/T^*)\exp(\Delta^*_{ab}/T) \qquad (5)$$

T^* is considered as the field-averaged superconducting transition temperature, while the temperature interval $T_c < T < T^*$ where the pseudogap state exists is defined by the

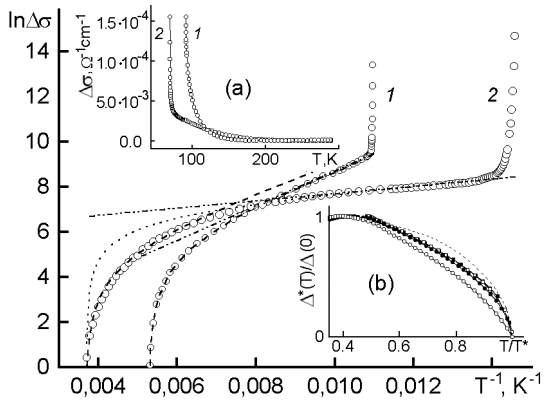

Fig. 3. Temperature dependences of the excess conductivity in the *ab*-plane for the K1 crystal in $\ln(\Delta\sigma) - 1/T$ and $\Delta\sigma - T$ [inset (a)] coordinates measured prior to and after the oxygen content reduction (curves *1* and *2*, respectively). Inset (b) presents the pseudogap temperature dependences in the $\Delta^*(T)/\Delta^*_{max} - T/T^*$ coordinates (Δ^*_{max} is plateau Δ^* value far from T^*). The open symbols are for K1 crystal data, the full ones, for K2. The curves denoted by squares were measured prior to the oxygen content reduction, those denoted by circles, after that. The otted line shows the $\Delta^*(T)/\Delta(0)$ vs. T/T^* dependence calculated in [13, 14].

rigidity of the order parameter phase which decreases as the oxygen deficiency increases. It is seen in Fig. 3 that the Δ^*_{ab} value is essentially temperature-independent far from T^* ($\Delta^*_{ab} = \Delta^*_{max}$) and becomes temperature-dependent quantity when approaching T^*:

$$\Delta^*_{ab}(T) \sim \Delta^*_{\max}(1 - T/T^*)^{1/2}. \qquad (6)$$

The $\Delta\sigma(T)$ dependence approximation by expressions (4), (5) and (6) is shown in Fig. 3 by dash-and-dot, dot and dash lines, respectively. In such a manner, using the methodology proposed in [5], the temperature dependence $\Delta^*_{ab}(T)$ can be constructed from the experimental curve $\ln\Delta\sigma$ up to the point T^*. Inset (b) in Fig. 3 show the temperature PG dependences in $\Delta^*(T)/\Delta_{max} - T/T^*$ coordinates (Δ_{max} is the plateau Δ^* value far from T^*). The $\Delta^*(T)/\Delta(0)$ vs. T/T^* dependence in this Figure are shown by the dotted line. The dependences were calculated according to [13, 14] using the average field approximation within the BCS-BEK crossover theoretical model, taking as the crossover pa-

rameter $\mu/\Delta(0) = 10$ (where μ is chemical potential of the carrier system; $\Delta(0)$, the energy gap value for $T = 0$). Taking into consideration the conventionality in determining the PG opening value T^* as a deviation from linearity in the $R(T)$ dependence, we may consider the experiment to agree well with the theory.

As is shown in Fig. 3, $\Delta\sigma$ increases sharply when approaching T_c. It is well known [15] that the excess conductivity near T_c is caused by the fluctuating pairing of carriers (FC) the contribution of which to the conductivity at $T > T_c$, regarding the two-dimensional (2D) and three-dimensional (3D) cases, are described by the equations:

$$\Delta\sigma_{2D} = \frac{e^2}{16hd}\varepsilon^{-1}, \quad (7)$$

$$\Delta\sigma_{3D} = \frac{e^2}{32h\xi_c(0)}\varepsilon^{-1/2}, \quad (8)$$

where $\varepsilon = (T - T_c)/T_c$; e is electron charge; $\xi_c(0)$ is the coherence length along **c** axis at $T \to 0$; and d, a characteristic size of the two-dimensional layer. As mentioned above, the T_c value was determined in our case in the maximum point of the $dR_{ab}(T)/dT$ dependence in the superconductive transition area corresponding to the high-temperature phase (Fig. 2).

In Fig. 4, the $\Delta\sigma(T)$ dependences are presented in $\ln\Delta\sigma(\ln\varepsilon)$ coordinates. In the temperature interval between T_c and $1.05 - 1.15T_c$ (depending on the oxygen concentration), these dependences are approximable well by straight line with a slope of $\mathrm{tg}\alpha_1 \approx -0.5$, in accordance to the power index $-1/2$ in the equation (8), thus evidencing the 3D character of fluctuating superconductivity within this temperature range. At the further temperature elevation, the $\Delta\sigma$ decline rate increases appreciably ($\mathrm{tg}\alpha_2 \approx -1$). This is an indication of the fluctuation conductivity (FC) dimensional change. Then, it follows from the equations (7) and (8) that at the 2D-3D crossover point,

$$\xi_c(0)\varepsilon_0^{-1/2} = d/2. \quad (9)$$

In this case, having determined the ε_0 value and using published data on the interplane distance dependence on δ [16] ($d \approx 11.7$ Å), we can calculate the the coherence length $\xi_c(0)$. As is shown in Table, the $\xi_c(0)$ value calculated according to (9), increases from 1.8–1.9 до 4.2 Å as T_c decreases, which is in agreement with $\xi_c(0)$ values obtained for YBaCuO samples with various oxygen concentrations [17].

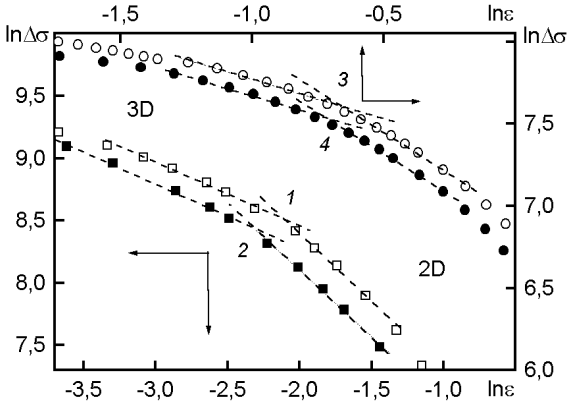

Fig. 4. Conductivity $\Delta\sigma(T)$ dependences in $\ln\Delta\sigma - \ln\varepsilon$ coordinates. The curves in are numerates as in Fig. 1. The dotted lines present the approximation at $\mathrm{tg}\alpha_1 \approx -0.5$ (3D regime) and $\mathrm{tg}\alpha_2 \approx -1.0$ (2D regime).

In summary, the main results of the present work are as follows. A decrease of the oxygen doping degree in the $HoBa_2Cu_3O_{7-\delta}$ single crystal results in a transition from the metallic behavior of temperature conductivity dependences along the axis **c** to the hopping conductivity with a variable length of hop. In the case of oxygen deficiency, phase transitions at 155 and 88 K change the activation energy of the charge transfer along the **c**-axis. In the *ab*-plane, the reduction of oxygen content results in a significantly narrowed linearity interval of $\rho_{ab}(T)$ dependence and in extended interval where the pseudogap regime is realized. The excess conductivity is described by exponential temperature dependence within a wide temperature range. When the oxygen content is varied, the absolute values of the in-plane and off-plane energy gaps (in the ab-plane, along **c**-axis) change, the signs of their derivatives being different. When the Δ_c increases, the pseudogap value Δ^*_{ab} decreases and vice versa. The theoretical model of crossover (BCS - BEK) provides a satisfactory description of the pseudogap temperature dependence. The shift towards lower critical temperature values for the superconducting transition for the ρ_c components as compared to ρ_{ab} may be a result of Fridel transition in the investigated samples.

References

1. M.A.Obolenskii, *Low Temp.Phys.*, **16**, 1103 (1990).
2. M.A.Obolenskii, *Low Temp.Phys.*, **23**, 882 (1997).
3. M.V.Sadovskii, *Usp. Fiz. Nauk*, **44(5)**, 515 (2001).
4. P.Pieri, G.C.Strinati, D.Moroni, *Phys.Rev. Lett.*, **89**, 127003 (2002).
5. D.D.Prokofyev, M.P.Volkov, Y.A.Boiko, *Fiz. Tverd.Tela*, **45(7)**, 1168 (2003).
6. B.P.Stojkovic, D.Pines, *Phys.Rev. B*, **55**, 8567 (1997).
7. B.L.Arbuzov, O.M.Bakunin, A.E.Davletishin et al., *Zh. Eksp. Teor. Fiz.*, **48**, 399 (1988).
8. V.N.Zverev, D.B.Shovkun, I.G.Naumenko, *Zh. Eksp. Teor. Fiz.*, **68**, 309 (1998).
9. J.Fridel, *J.Phys.(Paris)*, **49**, 1561 (1988).
10. M.Dzierzava, M.Zamora, D.Baeriswyl, X.Bagnoud, *Phys.Rev.Lett.*, **77**, 3897 (1996).
11. A.F.Prekul, B.A.Rassohin et al., *SFCT*, **3**, 381 (1990).
12. Anand Vyas, C.C.Lam, L.J.Shen, *Physica C*, **341** (2000).
13. E.Babaev, H.Kleinert, Cond-mat/9804206 (1998).
14. E.Babaev, H.Kleinert, *Phys.Rev.B*, **59**, 12083 (1999).
15. L.G.Aslamasov, A.I.Larkin, *Fiz.Tverd.Tela*, **10**, 1104 (1968).
16. G.D.Chryssikos, *Physica C*, **254**, 44 (1995).
17. M.A.Obolenskii, *Low Temp.Phys.*, **32**, 746 (2006).

Анізотропія провідності і еволюція псевдощілинного стану у монокристалах $HoBa_2Cu_3O_{7-\delta}$ із заданою топологією площинних дефектів при зниженні вмісту кисню

М.О.Оболенський, Р.В.Вовк, О.В.Бондаренко, І.Л.Гулатіс

Виміряно температурні залежності електропровідності вздовж осі **c** і в *ab*-площині монокристалів $HoBa_2Cu_3O_{7-\delta}$ з різним вмістом кисню. Визначено температурні залежності величини псевдощілини. Показано, що ці залежності задовільно описуються у межах теорії кросовера БКШ-БЕК. Посилення ефектів локалізації приводить до пригнічення псевдощілинного стану. Виявлено значну анізотропію надпровідних властивостей при вимірюванні температурних залежностей електроопору вздовж і поперек базисної площини.